Proceedings SPIE. Volume 12185, Adaptive Optics Systems VIII, 121850X (29 August 2022), 8p. + presentation
2022
https://doi.org/10.1117/12.2628885
https://archimer.ifremer.fr/doc/00801/91283/

The Phase-Shifted Zernike wave-front sensor

Cisse Mahawa [1, 2, *], Chambouleyron Vincent [1], Fauvarque Olivier [3], Bond Charlotte Z. [4], Levraud Nicolas [2, 5], Sauvage Jean -Francois [2], Neichel Benoit [1], Fusco Thierry [2]

[1] Aix Marseille Univ., CNRS, CNES, Lab. d'Astrophysique de Marseille (France)
[2] DOTA, ONERA, Univ. Paris Saclay (France)
[3] IFREMER, Lab. Detection, Capteurs et Mesures (LDCM) (France)
[4] UK Astronomy Technology Ctr. (United Kingdom)
[5] INAF, Osservatorio Astrofisico di Arcetri (Italy)

* Corresponding author : Mahawa Cisse, email address : mahawa.cisse@lam.fr

Abstract :

The next generation of Giant Fragmented Telescopes will allow the study of faint and distant objects such as exoplanets. But the structure of the telescope also brings new challenges such as pupil fragmentation or Low-Wind Effect (LWE) that needs to be corrected by the Adaptive Optics (AO) system. The Wave-Front Sensor (WFS) which is the heart of the AO system needs to be able to measure these aberrations. Because of its high sensitivity, the Zernike Wave-Front Sensor (ZWFS) appears to be a viable candidate as a 2nd stage instrument to measure telescope seeing or differential piston. However, its use is limited by its small dynamic range. We propose here a new concept of WFS based on the ZWFS with a better dynamic range : the Phase Shifted ZWFS (Phase-Shifted ZWFS).

Keywords : Giant telescopes, adaptive optics, wave-front sensor, high performance, data fusion

1. INTRODUCTION

With the advent of the Extremely Large Telescopes (ELT), the structure of the telescope itself induces perturbations and limits the resolution of the instrument. In order to achieve high angular resolution, we need to be able to correct the telescope aberrations such as dome seeing or petalling. These low order frequency aberrations need to be corrected within the AO loop so with the atmospheric turbulence. Classical AO systems are unable to correct these aberrations. For example, on the Very Large Telescope, the LWE was measured by the ZELDA which is a Zernike based WFS because the Shack-Hartmann of the AO system was unable to measure the phase discontinuity characteristics of the LWE.[1]

The ZWFS which is already used for high-contrast imaging to correct low-wind effect and NCPA is a potential candidate to for this type of aberrations because of its high sensitivity.[1] Indeed, this WFS is more sensitive than the PWFS.[2] Its higher sensitivity comes at the cost of a small linearity range which makes its use more complicated.

The goal of this paper is to introduce the Phase-shifted ZWFS which is a Zernike based WFS with a higher dynamic range than the classical ZWFS. This sensor was proposed by David S.Doelman as the Vector-Zernike phase mask.[3] Improving the dynamic of the ZWFS will allow to take advantage of the high sensitivity of the ZWFS to improve the correction of the first AO stage and have a WFS able to measure LWE or petalling. First we are going to point out the dynamic range of the ZWFS (section 2). The we will introduce the concept of the Phase-Shifted ZWFS (section 3).

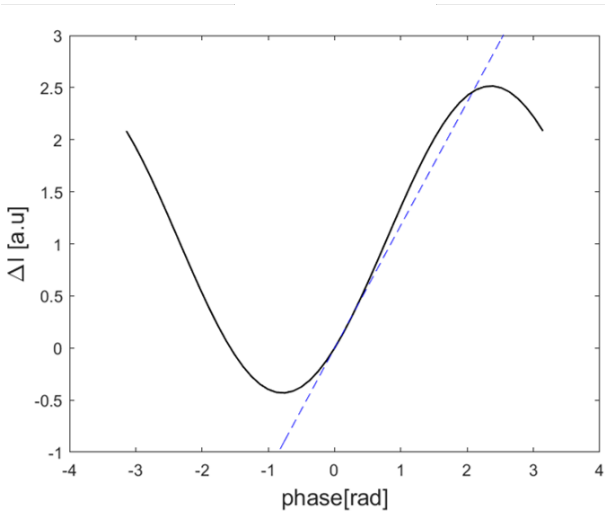

Figure 1: Reduced intensity of a pixel. $\Delta I = I(\Phi) - I_0$- where I_0 is the reference intensity obtain for a flat wave-front. The black curve is the reduced intensity of the pixel, the blue one is the linear phase re-constructor

2. DYNAMIC OF THE ZWFS

The dynamic of a sensor characterises its linear regime. Working on the linear regime of the sensor allows to use the classical formalism of the interaction matrix to invert the system and have a phase estimation from the data given by the sensor. In the case of the ZWFS the inversion process is simpler because we know the analytical expression of the intensity on the detector as a function of the phase.[4] The intensity can be express as follow:

$$I(\Phi) = \mathbb{I}_p^2 + \frac{1}{2} + \mathbb{I}_p(\sin(\Phi) - \cos(\Phi)) \tag{1}$$

Where $\mathbb{I}_p$ is the pupil function.

With the expression of the intensity on the detector we can built two different phase re-constructors. These re-constructors describe the operating of the ZWFS in the small phase regime.[5]

2.1 Dynamic of the classical ZWFS

To describe the behaviour of the ZWFS with respect to the phase, we put a flat wave-front in the pupil plane and we modify the intensity on only one pixel. The reduced intensity curve is plotted in Figure 1. From this plot we can exhibit one linear phase re-constructor cf equation 2, which will give an accurate phase estimation only for small phases, and one non linear re-constructor using the arcsin function. This will provide a dynamic range of π. However, when doing phase estimation, we are not only considering one pixels but a $2D$ phase map. That is why the best approach to quantify the dynamic of a WFS is to study its dynamics range with respect to a modal basis. This is shown in the next subsection for the Zernike basis.

$$\Phi = I(\Phi) - \frac{1}{2} \tag{2}$$

2.2 Example with a Tip

The linearity curve of the ZWFS for a given mode gives a concrete idea of the linearity range of the sensor. As an example, we plot in Figure 2 the linearity curve of the ZWFS obtained for a tip mode. This curve highlights the dynamic range of the ZWFS for this mode which is between [-0.4;0.4] phase amplitude in rad RMS. Outside of the linearity domain, the inversion process which is a linear process is no longer accurate. For example, if we have a tip of amplitude 0.88 rad RMS in the pupil plan, the estimated phase is not a perfect tip. The first

interesting point is that the amplitude of the tip of the estimated phase is lower than the one of the input phase cf Figure 3c. This difference is due to the optical gain. The second point is that others Zernike mode appears after the inversion process. This modal confusion is due to the non-linear intensities of the ZWFS which now prevail on the linear intensity. The plot here highlights the difficulties of the ZWFS to properly estimate big phase amplitude.

2.3 Impact of the phase residuals on the inversion process

In this section we will point out the impact of the phase residuals in the linearity range of the ZWFS. The simulations are done with the following parameters: a 1m telescope with 128 pixels in the diameter, a modal deformable mirror (DM) correcting 100 modes and a r_0 of 25cm. The goal of this simulation was to add a tip to the turbulent point spread function and retrieve the tip by using the linear phase re-constructor. Figure 4 shows the simulations results. We notice a strong decrease of the sensitivity in presence of phase aberrations. Although the Strehl ratio is equal to 33%, the tip will be strongly under-estimated. This figure highlights the difficulties of the ZWFS to measure specific aberrations in presence of phase residuals because of its small dynamic range and the strong loss of sensitivity.
To use this sensor to measure specific aberrations in presence of phase residuals, one needs to works in a almost

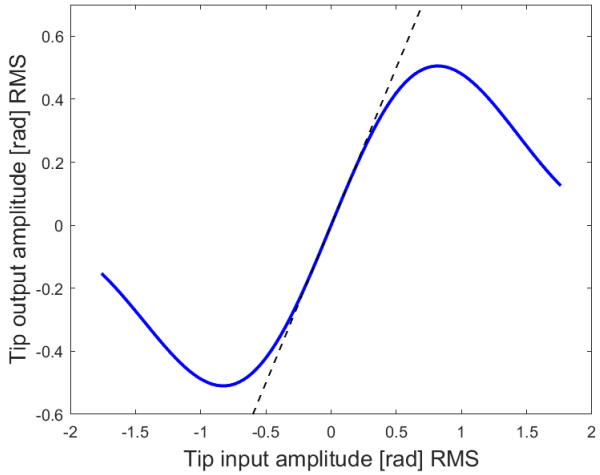

Figure 2: Linearity curve of the ZWFS for the Zernike mode Z_2. The inversion process is done with the analytical expression of the intensity as a function of a phase

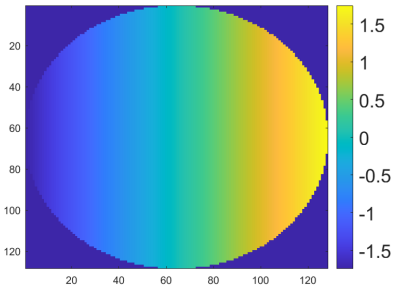

(a) Input phase amplitude of 0.88 rad RMS

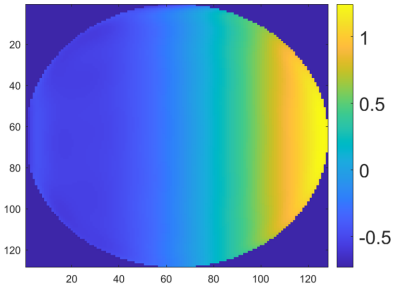

(b) Estimated phase: RMS error of 0.41 rad

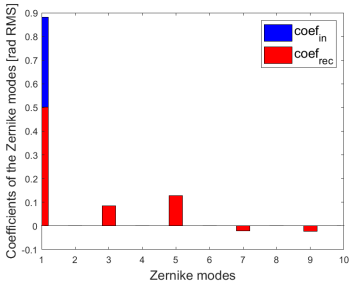

(c) Projection of the estimated phase on the first 10 Zernike modes

Figure 3: The input phase (left), the estimated phase (middle) and the projection of the phase on the Zernike modes (right) are presented. The amplitude of the input phase was chosen outside of the linear range of the ZWFS.

limited diffraction regime which means to work as a 2^{nd} stage AO. The 1^{st} stage AO system aim to achieve a high level of correction in order for our 2^{nd} stage sensor to refine the correction by correcting the AO residuals and the aberrations induced by the telescope itself such as LWE or petal modes.

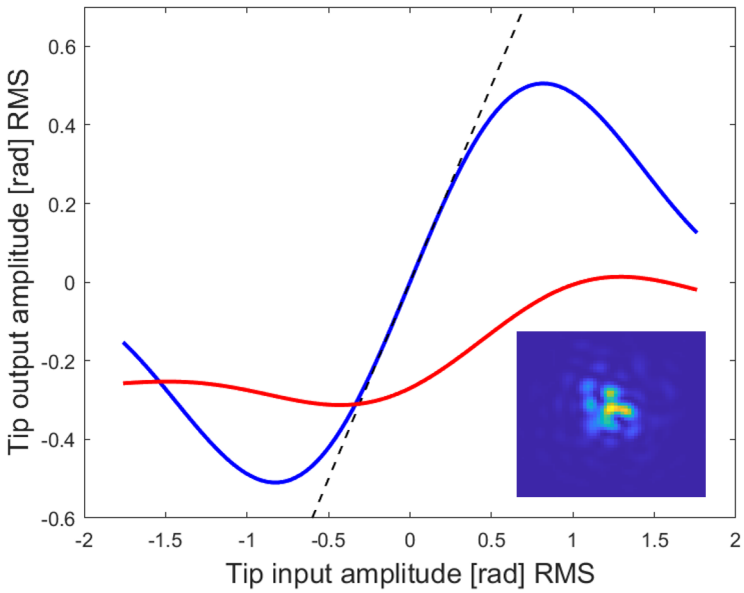

Figure 4: Linearity curve of the ZWFS for the Zernike mode Z_2. The inversion process is done with the analytical expression of the intensity as a function of a phase. The blue curve is the phase obtain without aberration. The red one is with phase aberration

3. THE PHASE-SHIFTED ZWFS

The ability of the ZWFS to measure LWE is not to be proven.[1] However, the phase estimation, process is limited by the non-linearities of the sensor cf section 2. In order to facilitate and improve the phase estimation in a phase residual regime, one need to improve the dynamic range on the sensor without losing in sensitivity.
The optical set-up presented here is to compare to the one developed by David S.Doelman the Vector-Zernike Phase mask.[3] What we presente here is a the study of the dynamic of such a phase mask compare to the classical ZWFS.

3.1 Optical set-up

The following optical set-up allows to increase the dynamic range of our ZWFS. We combine two Zernike masks, one of diameter equal to $1.06\frac{\lambda}{d}$ and a depth of $\frac{\pi}{2}$ named Z_+ and the second one with the same diameter but a depth of $-\frac{\pi}{2}$ Z_- cf Figure 5. A similar optical device was proposed by David.S Doelman[3]
The optical set-up on Figure 5 is a classical Fourier Filtering Wave-front Sensor optical scheme. After the pupil plan we have a Wollaston that divide the two polarizations of the light. The two collimated beam are focused on the focal plan of a lense were we put the two ZWFS, Z_+ and Z_-. Then we reimage the pupil thanks to a lense on the detector. Using a Wollaston allow us the image the two pupils images given by the two masks by using only one detector. By doing this we use two times more pixels for the measurements which will double the Read-Out-Noise, but because we are using the same amount of photons, the photon noise will remain the same.

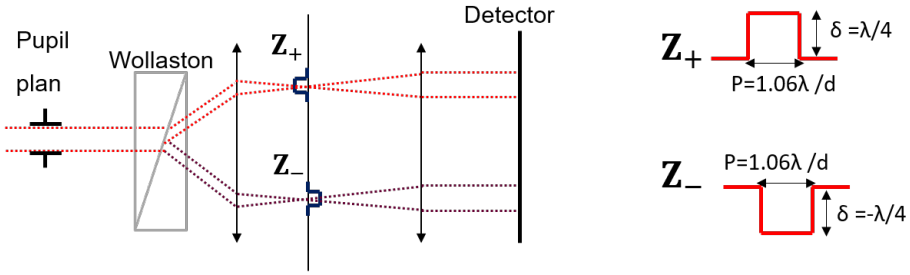

Figure 5: Opical set-up of the Phase-Shifted ZWFS

3.2 Dynamic improvement

The 2^{nd} ZWFS is the transconjucated of the first one. The intensity on the detector corresponding to each mask can be written as follow cf equation 1:

$$\begin{aligned} I_+(\Phi) &= \mathbb{I}_p^2 + \frac{1}{2} + \mathbb{I}_p(\sin(\Phi) - \cos(\Phi)) \\ I_-(\Phi) &= \mathbb{I}_p^2 + \frac{1}{2} - \mathbb{I}_p(\sin(\Phi) + \cos(\Phi)) \end{aligned} \tag{3}$$

By doing linear combination of the equation I_+ and I_-, one can have access to the sine and the cosine of the phase cf equation 4. We now use a new phase re-constructor the *atan* function which give the system a dynamic of 2π.

$$\begin{aligned} \sin(\Phi) &= \frac{I_+(\Phi) - I_-(\Phi)}{2\mathbb{I}_p} \\ \cos(\Phi) &= \frac{2\mathbb{I}_p^2 + 1 - (I_+(\Phi) + I_-(\Phi))}{2\mathbb{I}_p} \end{aligned} \tag{4}$$

3.3 Comparison between the classical ZWFS and the Phase-Shifted ZWFS in a phase residual regime

The aim of this section is to compare the phase estimation of the classical ZWFS and the one given by the Phase-Shifted ZWFS. First we will show the phase estimation given by the two WFS for a small phase aberration then we will deal with the petal measurement in presence of phase residuals.

3.3.1 Small phase regime

The input phase is an atmosphere turbulence like phase but of very small amplitude: 1 rad RMS and a Peak-to-Valley amplitude of 5.6rad. The idea was to evaluate the capacity of the Phase-Shifted ZWFS to measure a phase aberrations containing several modes. Figure 6 shows the results of the inversion process for both masks. The phase amplitude was chosen to be outside the linearity domain of the ZWFS but inside the one of the Phase-Shifted ZWFS. Because along the linear range of the classical ZWFS both sensors give the same phase estimation.

The results plotted in Figure 6 shows that the estimated phase obtained with the ZWFS is less accurate than the one given by the Phase-Shifted ZWFS. Indeed, the estimation given by the ZWFS present sign inversion (cf black circle in the Figure 6b) which can make the AO loop diverge. With the Phase-Shifted ZWFS, the estimation is more accurate. The shape of the estimated phase is similar to the one of the input phase, we do not see area with sign inversion. Furthermore, the RMS error is reduced with by a factor of 40% which means that the AO loop will converge more rapidly. The result given by the Phase-Shifted ZWFS can be improve by

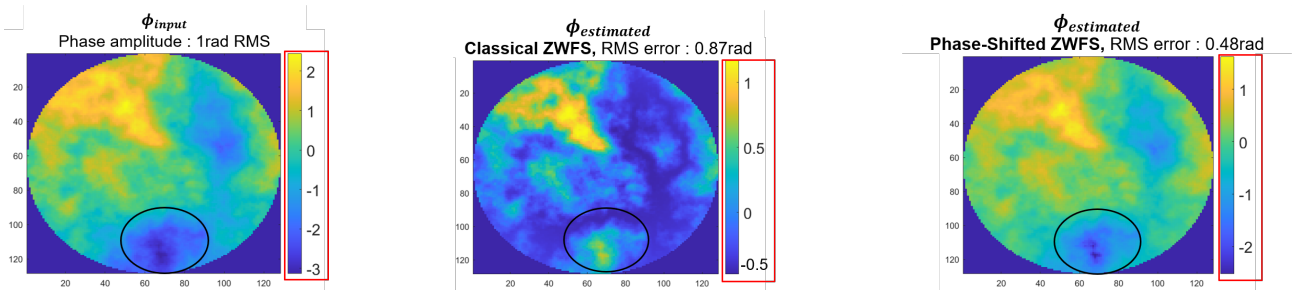

(a) Input phase (b) Classical ZWFS (c) Phase-Shifted ZWFS

Figure 6: Comparison of the phase estimation given by the classical ZWFS (middle) and the one given by Phase-Shifted ZWFS (right) in a small phase regime

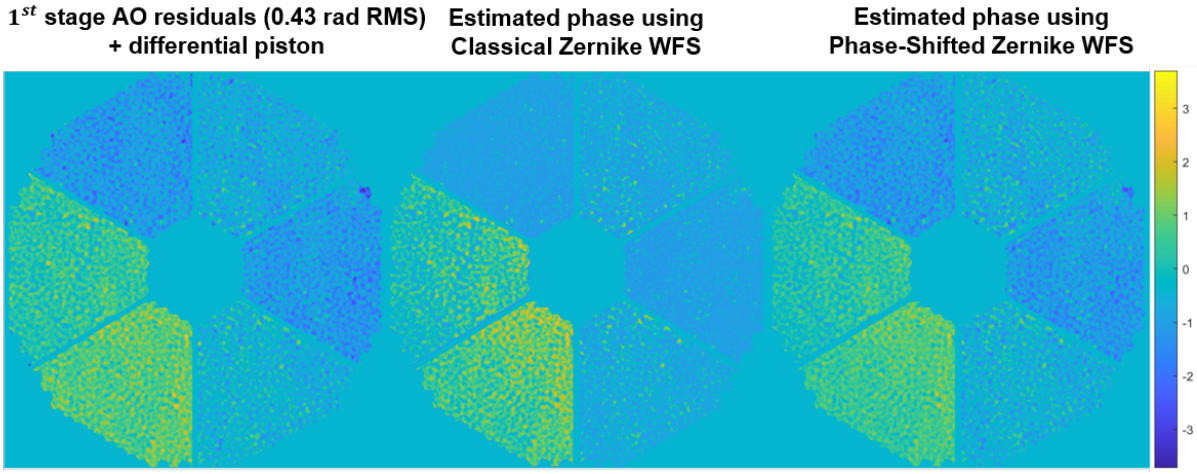

Figure 7: Piston estimation in presence of phase residuals. Left: input phase, Middle: Estimation given by the ZWFS, Right: Estimation given by the Phase-Shifted ZWFS

implementing data fusion and using a gain scheduling camera to compute the optical gains thanks to a camera on the focal plane.[6] The computation of the optical gain is not the main subject of this paper but can be done by either using the convolutional approach[7] or using an interaction matrix computed around the the residual phase.

An other point is that because of the less accurate phase estimation due to area where the sign is not properly estimated, computing the optical gain for the classical ZWFS will amplify this effect and make the AO loop diverge more quickly. Which is the total opposition of what we want. The results presented here give us a confident in our Phase-Shifted ZWFS. With its larger dynamic range, the sensor is able to provide a better phase estimation than the classical ZWFS.

3.3.2 Petal estimation in presence of phase residuals

Here we confront the estimation of the petal modes in presence of phase residuals given by the two different phase masks. The characteristics of the simulation are the following: a ELT like pupil, phase residuals amplitude of 0.43 rad RMS to which we add piston modes cf Figure 7. The plots of the errors maps given by Figure 8 show that the ZWFS struggles to properly estimate the differential piston between each fragment. We also notice area were the sign is inverted cf Figure 8a. Although by using the Phase-Shifted ZWFS differential piston is correctly estimated. We have a better piston estimation, phase estimation and no sign inversion cf Figure 8b.

The Phase-Shifted ZWFS provide a more accurate and robust estimation of the differential piston and of the phase residuals than the classical ZWFS thanks to its bigger linearity range. The RMS error is reduced by a factor of 10% with this sensor.

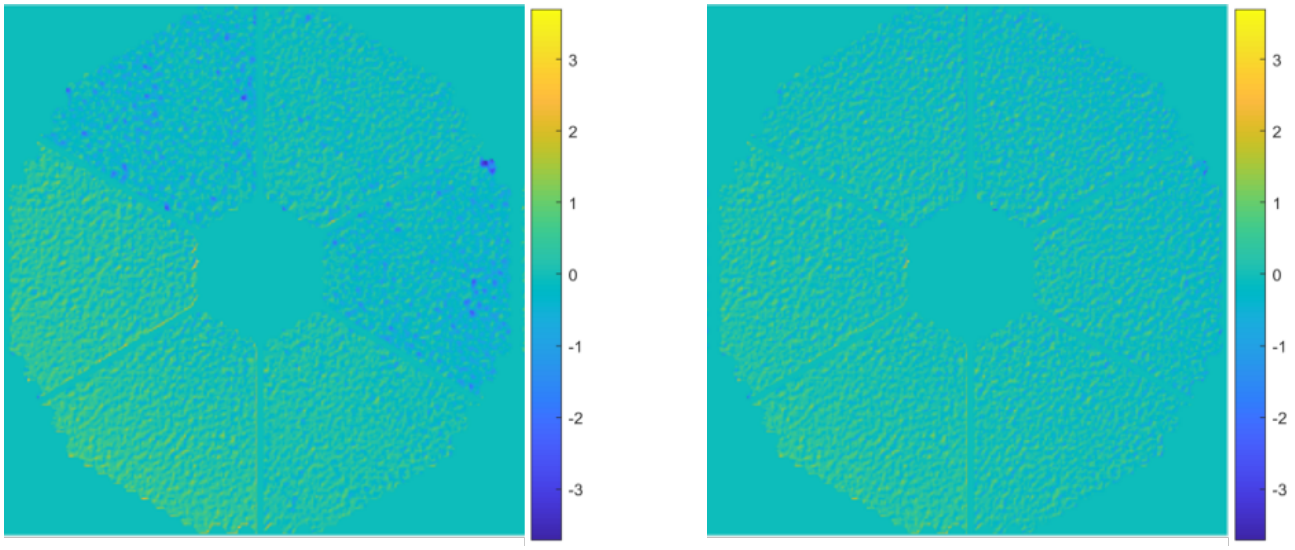

(a) Classical ZWFS (b) Phase-Shifted ZWFS

Figure 8: Error maps of the phase estimations obtained by subtracting the estimation given by the phase masks to the input phase

4. CONCLUSION AND PERSPECTIVES

The aim of this study was to exploit the high sensitivity of the ZWFS and use it to measure aberrations such as LWE of petal modes. To do so one needs a better linearity range of the sensor in order to use it in a phase residual regime.
Therefore, the study was focus on a way to improve the dynamic range of the classical ZWFS and to do so we studied the dynamic of the Phase-Shifted ZWFS. This sensor combines two Zernike masks transconjucated one another.
The optical set-up proposed allows to limits the sensitivity loss in terms of photon noise though we divide by two the sensitivity with respect to the Read-Out-Noise.
The Phase-Shifted ZWFS has a better dynamic range than the classical ZWFS which allows to perform a better measurement of the phase aberrations. Indeed, this sensor is as good at measuring multimodal aberrations as it is at measuring differential piston in the presence of 1^{st} stage AO residuals. The simulations results shown in this study show that the Phase-Shifted ZWFS is a possible candidate for a 2^{nd} stage AO. And using this sensor will allow to work in a less restrictive phase residuals regime thanks to its better dynamic range and to converge more quickly than the classical ZWFS.

The next step of the simulations will be to optimise the Phase-Shifted ZWFS by first modifying the shape of each Zernike masks. A study will by done to quantify the impact of the diameter of the Zernike mask on the AO performance. We will also deal with the non-linearities of this sensor that remains by implementing the calculation of the optical gain to improve the measurement of the sensor. We also think about using machine-learning to deal with the modal confusion and test this method to estimate the phase.

After the optimisation of this phase mask, will will implement it on the Loops bench[8] to have experimental results.

ACKNOWLEDGMENTS

This work benefited from the support of the the French National Research Agency (ANR) with WOLF (ANR-18-CE31-0018), APPLY (ANR-19-CE31-0011) and LabEx FOCUS (ANR-11-LABX-0013); the Programme In-

vestissement Avenir F-CELT (ANR-21-ESRE-0008), the Action Spécifique Haute Résolution Angulaire (ASHRA) of CNRS/INSU co-funded by CNES, the ECOS-CONYCIT France-Chile cooperation (C20E02), the ORP H2020 Framework Programme of the European Commission's (Grant number 101004719) and STIC AmSud (21-STIC-09).

REFERENCES

[1] Milli, J., Kasper, M., Bourget, P., Pannetier, C., Mouillet, D., Sauvage, J.-F., Reyes, C., Fusco, T., Cantalloube, F., Tristam, K., et al., "Low wind effect on vlt/sphere: impact, mitigation strategy, and results," in [*Adaptive Optics Systems VI*], **10703**, 752–771, SPIE (2018).

[2] Chambouleyron, V., Fauvarque, O., Sauvage, J.-F., Dohlen, K., Levraud, N., Vigan, A., N'Diaye, M., Neichel, B., and Fusco, T., "Variation on a zernike wavefront sensor theme: Optimal use of photons," *Astronomy & Astrophysics* **650**, L8 (2021).

[3] Doelman, D. S., Auer, F. F., Escuti, M. J., and Snik, F., "Simultaneous phase and amplitude aberration sensing with a liquid-crystal vector-zernike phase mask," *Optics letters* **44**(1), 17–20 (2019).

[4] Janin-Potiron, P., N'Diaye, M., Martinez, P., Vigan, A., Dohlen, K., and Carbillet, M., "Fine cophasing of segmented aperture telescopes with zelda, a zernike wavefront sensor in the diffraction-limited regime," *Astronomy & Astrophysics* **603**, A23 (2017).

[5] N'Diaye, M., Dohlen, K., Fusco, T., and Paul, B., "Calibration of quasi-static aberrations in exoplanet direct-imaging instruments with a zernike phase-mask sensor," *Astronomy & Astrophysics* **555**, A94 (2013).

[6] Chambouleyron, V., Fauvarque, O., Sauvage, J.-F., Neichel, B., and Fusco, T., "The focal-plane assisted pyramid wavefront sensor: enabling frame-by-frame optical gains tracking," *arXiv preprint arXiv:2103.02297* (2021).

[7] Fauvarque, O., Janin-Potiron, P., Correia, C., Brûlé, Y., Neichel, B., Chambouleyron, V., Sauvage, J.-F., and Fusco, T., "Kernel formalism applied to fourier-based wave-front sensing in presence of residual phases," *JOSA A* **36**(7), 1241–1251 (2019).

[8] Janin-Potiron, P., Chambouleyron, V., Schatz, L., Fauvarque, O., Bond, C. Z., Abautret, Y., Muslimov, E., El-Hadi, K., Sauvage, J.-F., Dohlen, K., et al., "Adaptive optics with programmable fourier-based wavefront sensors: a spatial light modulator approach to the loops testbed," *arXiv preprint arXiv:1903.06599* (2019).